A Slot Model for Loss Estimation in Superconducting AC Electrical Machine Windings

Original
A Slot Model for Loss Estimation in Superconducting AC Electrical Machine Windings / Santos Perdigao Peixoto, I., Perilli, L., Graffeo, F., Fernandes, J.F.P., Da Costa Branco, P.J., Vaschetto, S.. - (2024), pp. 1-7. (International Conference on Electrical Machines Torino 1-4 September) [10.1109/ICEM60801.2024.10700257].

Availability:
This version is available at: 11583/2993311 since: 2024-10-10T18:26:45Z

Publisher:
IEEE

Published
DOI:10.1109/ICEM60801.2024.10700257

(Article begins on next page)

A Slot Model for Loss Estimation in Superconducting AC Electrical Machine Windings

Inês S. P. Peixoto, *Student Member, IEEE*
Politecnico di Torino
Dipartimento Energia
Turin, Italy
ines.peixoto@polito.it

Lorenzo Perilli, *Student Member, IEEE*
Politecnico di Torino
Dipartimento Energia
Turin, Italy
lorenzo.perilli@polito.it

Federica Graffeo, *Member IEEE,*
Politecnico di Torino
Dipartimento Energia
Turin, Italy
federica.graffeo@polito.it

João F. P. Fernandes, *Member, IEEE*
IDMEC, Instituto Superior Técnico
University of Lisbon
Lisbon, Portugal
joao.f.p.fernandes@tecnico.ulisboa.pt

Paulo J. da Costa Branco, *Member, IEEE*
IDMEC, Instituto Superior Técnico
University of Lisbon
Lisbon, Portugal
pbranco@tecnico.ulisboa.pt

Silvio Vaschetto, *Senior Member, IEEE*
Politecnico di Torino
Dipartimento Energia
Turin, Italy
silvio.vaschetto@polito.it

***Abstract*— The use of superconducting AC windings in rotating electrical machines is usually avoided due to the non-negligible hysteresis losses of superconductors. However, if these AC losses are mitigated, their implementation may allow to further increase the power density of electrical machines. This paper proposes a methodology for evaluating the AC losses in superconducting tapes when applied to the realization of slotted stator windings in AC electrical machines. In particular, the approach allows to reduce the computational requirements when the geometrical nature of the considered superconducting electrical machine requires 3D finite-element models, as in the case of axial flux machines. The machine is first simulated with a 3D FEM model without superconductors. Then, using a 2D single-slot FEM model, the superconducting AC losses are computed. The methodology is applied to a case study of an axial flux permanent magnet machine with AC superconducting stator windings. The model is validated by comparing the magnetization and the transport current losses estimated in the superconductors by the FEM simulations with those by analytical formulations.**

Keywords—electrical machines, power density, superconductors, finite element method, T-A formulation.

I. INTRODUCTION

High-temperature superconductors (HTS) have started to be investigated as potential alternatives to conventional conductors in energy applications. The reason is that their high current carrying capacity and near-zero power loss in DC conditions make them particularly attractive for the realization of low-weight, high-power energy conversion devices. The expectation that higher power densities can be attained with superconducting electrical machines has also led in recent years to several funded projects for transportation and energy generation. Demonstrating prototypes were developed for offshore wind generators [1] – [3]. For transportation electrification, there has been a growing interest in propulsion motors for future electrified aircraft [4] – [6].

Superconducting machines can be built in both partially and fully superconducting configurations [7]. In the former one, the superconductors (SCs) are integrated into either the stator or the rotor of the machine.

Conversely, fully superconducting machines utilize SCs in both the rotor and stator circuits. These superconducting materials are commonly used as tape or wire coils in substitution of conventional copper conductors or magnetized bulks to replace permanent magnets [8].

Most of the superconducting AC electrical machines developed to date feature a partial configuration, where the superconducting circuits are restricted to the rotor side and carry DC currents for the machine excitation due to having intrinsic near-zero resistivity in DC conditions [9]. However, using SCs on the rotor implies significant challenges to keep them at cryogenic temperatures, such as adopting rotating cryocoolers. These drawbacks could be overcome if SCs were applied to the armature conductors located on the machine stator. However, in the armature windings of AC machines, the SCs are supplied with time-varying currents and are exposed to variable magnetic fields. Such operative conditions bring the SCs to manifest non-negligible hysteresis loss [10].

The accurate estimation of superconducting AC losses is essential for realizing practical designs of electrical machines with superconducting windings. The cryocooler must deliver the required cooling power to extract the heat incurred by the windings and maintain the superconductors within cryogenic temperatures. Indeed, excessive heating of the SC coils risks the disruption of the superconducting state, potentially causing irreversible damage to the SCs.

Different formulations can be found in the literature to estimate losses in the SCs and account for both the superconductor non-linear resistivity and its dependence on the surrounding magnetic fields [11], [12]. However, great detail is imperative to accurately compute power losses in superconducting materials. The tiny dimensions of SCs, together with their high width over thickness aspect ratio, make these non-linear models usually complex and computationally demanding to be applied in finite element method (FEM) simulations of rotating electrical machines [13]. This complexity is further exacerbated if 3D geometries and moving meshes are mandatorily required, such as for the design and analysis of axial flux machines. This would make machine design optimization processes requiring several FEM simulations highly impractical.

In order to provide more expedited methods compatible with machine design methodologies, the authors proposed in [14] a 2D single-slot model suitable for SC loss computation and application assessment in armature windings of axial flux superconducting machines.

This study was carried out within the "Superconducting electric machines and crYogenic power electronics for high efficiency, reliable and power-dense eNERGY conversion (SYNERGY)" project – funded by European Union – Next Generation EU within the PRIN 2022 program (D.D. 104 02/02/2022 Ministero dell'Universita e della Ricerca). This manuscript reflects only the authors' views and opinions, and the Ministry cannot be considered responsible for them.

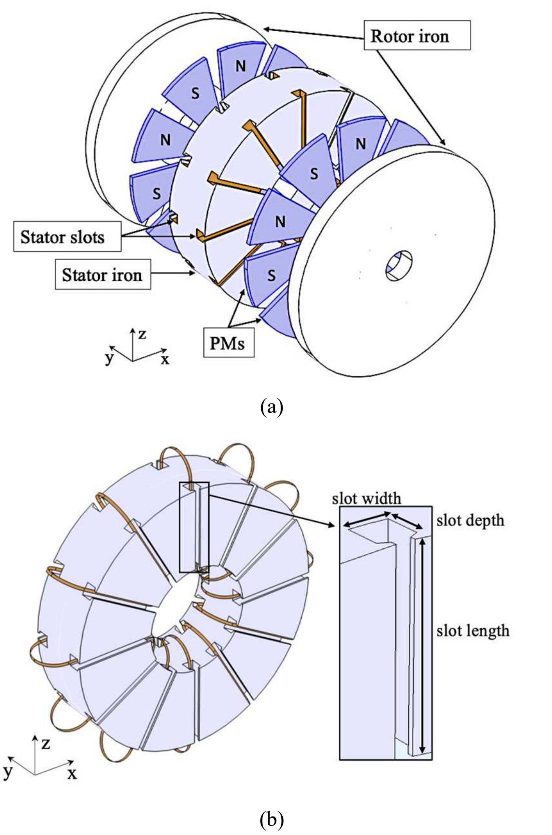

Fig. 1. Case study AFPM machine: (a) 3D sketch of the 10-pole 12-slot single-stator double-rotor configuration, (b) stator with core-wound tapes.

The approach consists of an initial simulation of the 3D machine model with standard copper conductors. By the magnetic field in the air gap and stator back iron regions, the spatial variation of the magnetic field on the slot edges is derived and applied to the 2D slot model, where the conductors are modeled using the superconducting formulations. In [14], the temporal evolution of the magnetic field in the 2D model is included by considering only the first time harmonic of the magnetic field spatial distribution.

This paper proposes an improvement of the method presented in [14], considering the magnetic field spatial distribution and temporal evolution at each mesh point of the slot boundaries. In this way, the 2D slot model replicates the magnetic field surrounding the SC coils of the 3D machine model more accurately. As in [14], the SCs are also modeled using a thin-sheet approximation with the T-A formulation.

II. Multi-Stage Axial Flux PM Machine Case Study

To evaluate the applicability and accuracy of the proposed methodology, a 10-pole 12-slot axial flux permanent magnet (AFPM) machine with core-wound coils is considered as a case study. Fig. 1a shows the 3D sketch for the considered multi-stage machine configuration, having a single-stator and double-rotor with permanent magnets.

Figure 1b presents a detail of the stator core with an example of conducting tapes positioned in a core-wound configuration. This machine type and winding layout have been selected for this case study because they may allow an easier future prototype realization for reduced machine dimensions.

TABLE I. Main Design Data of the AFPM Machine

Parameters	Values
Rated power (kW)	20
Rated speed (rpm)	1200
Magnet thickness (mm)	8
Magnet polar pitch (p.u.)	0.778
Airgap thickness (mm)	1
Outer Diameter (mm)	375
Inner Diameter (mm)	150
Total Axial length (mm)	164

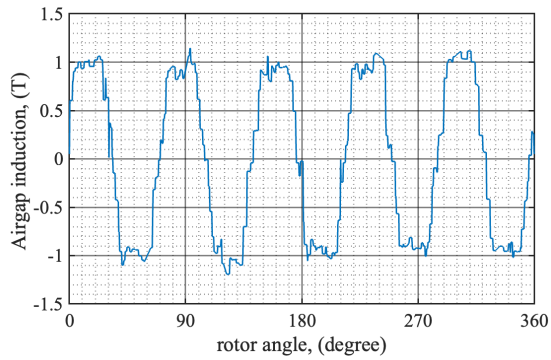

Fig. 2. Air gap flux density in rated load condition.

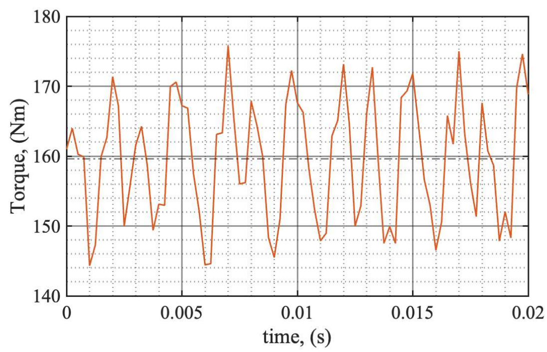

Fig. 3. Electromagnetic torque of the AFPM machine with copper windings.

Indeed, one of the drawbacks of superconducting tapes is their limited bending radius, which must be respected to preserve their mechanical integrity and electromagnetic properties. From this perspective, conventional distributed winding layouts are not the best option for applying SCs, mainly because of the multiple overlaps among the end-windings that make the conductors path not always straightforward. On the other hand, it is expected that toroidal windings present less criticalities on the bending radii, both at the inner and outer machine diameters. Moreover, the multi-stage axial flux machine with single-stator double-rotor configuration allows exploiting both sides of the toroidal winding layout.

For this study, both tooth and core winding layouts could have been chosen to respect the superconductors bending limitations. However, core wound coils (as shown in Fig. 1b), were considered more suitable to limit slot leakage perpendicular magnetic flux hitting the SC tapes surfaces, which heavily impacts the conductor performance and hysteresis losses.

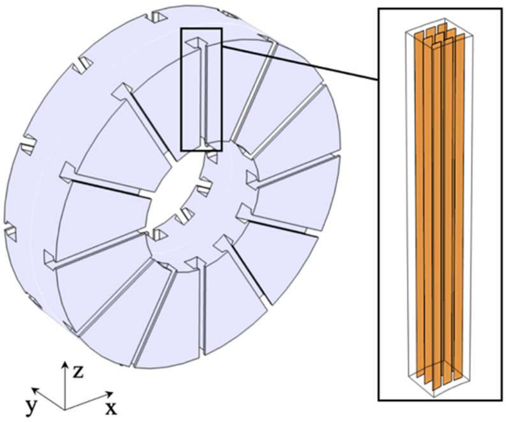

Fig. 4. FEM model of the stator core and a detail of the slot with the surface elements used to model the conductors.

Table I lists the main data for the AFPM considered for this research activity. It has to be remarked that this machine has been designed by the authors using conventional sizing equations for copper wounded axial flux machines [15]. It can therefore be considered as a case study for applying the superconducting formulations, as well as for the development and validation of the proposed modeling approach and of the AC loss estimation in the superconductors. However, further design refinements and optimization, that are beyond the scope of this paper, will be required for a prototype realization.

The overall performance of the sized machine has been verified by means of 3D FEM simulations with copper conductors. The 3D study was carried out using a copper wound armature, due to the high computational time required to simulate the same machine with superconducting coils for the intrinsic computational complexity introduced by the SCs formulations. In the developed FEM model, the copper conductors are here modeled as '*flat*' current conducting elements having the same dimensions as the SC tapes (see Fig. 4). In this way, the resulting magnetic field distribution into the slot is expected to be more consistent with that generated by superconducting tapes carrying the current. It goes without saying that this similarity is valid for simulations only, since copper conductors having the same dimensions as the SC tapes would not be suitable to transport the same current values.

The air gap flux density results in rated load condition and the electromagnetic torque obtained by the 3D model of the AFPM machine with copper conductors are shown in Fig. 2 and Fig. 3, respectively. The conducted FEM simulations are performed with all the current imposed in the q-axis, i.e., in maximum torque condition. Note that since the current is imposed in the armature coils in this model, the main difference between the superconducting and the copper machine models are the conductor losses and the resulting phase voltage for the same phase current.

For the 2D slot model simulations, superconducting REBCO tapes are considered, and their defining parameters are stated in Table II [16]. The tape width and height listed in the table refer to the geometrical dimensions of the whole coated tape. The thickness of the superconducting layer is 1.6µm only, as depicted in Fig. 5.

For the machine considered on case study, the maximum slot current at rated performance is equal to 910 A.

TABLE II. REBCO COATED CONDUCTOR PARAMETERS AT 77K

I_{c0} (A)	B_0 (mT)	n	Tape width (mm)	Tape height (µm)
162	140	21	4.01	95.6

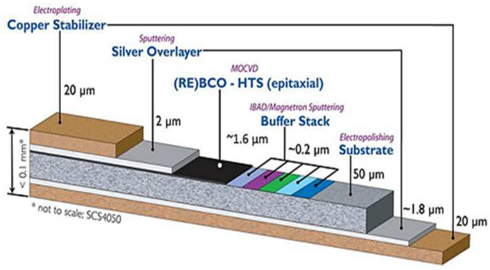

Fig. 5: Sketch of a coated SC REBCO tape [16].

Therefore, to limit the current in each conducting element well below the critical current value for the considered REBCO tape (see Table II), it has been assumed that each slot has 9 conductors, as illustrated in Fig 4.

III. SUPERCONDUCTOR MODELING

A. *Superconducting state characteristics*

Superconductors are characterized by three main parameters, dependent on the material: a critical temperature T_c, a critical magnetic field H_c, and a critical current density J_c. Surpassing any of these critical values causes the loss of the superconducting state.

In FEM, the relations (1) and (2) are defined on the superconducting domains to characterize the material behavior. In detail, the critical current density dependence on the applied magnetic flux density is introduced through the Kim model in (1) [17].

$$J_C(B) = \frac{J_{c0}}{1+|\mathbf{B}|/B_0} \tag{1}$$

In (1), J_{c0} is the critical current density in self-field conditions, and B_0 is the magnetic flux density that lowers the critical current density J_c by half. Both these constants depend on the tape materials. Usually, they are provided by the manufacturer, or they can be obtained through experimental tests on samples of the SC tape.

The non-linear relation between the electric field and the current density in superconductors is defined in (2) through the *E-J* power law [18].

$$\boldsymbol{E} = \rho_{sc}\mathbf{J} = E_0\left(\frac{|\mathbf{J}|}{J_C(\mathbf{B})}\right)^{(n-1)}\mathbf{J}/J_c(\mathbf{B}) \tag{2}$$

In (2), E_0 is the critical electric field, defined by convention as 100 µV/m, and n is the superconducting exponential constant, which defines the steepness of the transition between the superconducting and resistive state (that can also be interpreted as a measure of tape quality). Notice that to estimate the AC losses, the critical current density dependence on the temperature is not considered in this model, and the temperature is assumed to be constant at 77 K.

B. *T-A formulation*

Although coated conductors consist of multiple layers [19], the model applied in this study adopts the thin-sheet approximation. It is assumed that all the current in the tape flows exclusively in the superconducting layer, which provides the lowest resistivity path.

Thus, the tape structure is simplified to a single SC layer of negligible thickness, i.e., a surface in 3D models or a line in 2D models. Consequently, layers such as copper, silver, and the substrate (steel) are excluded from the FEM model.

This approximation applies to REBCO tapes due to their high aspect ratio (see Table II), thereby enabling the assumption that all the current flows tangentially to the tape surface [20], [21]. In the literature, it was verified that the thin-sheet approach remains valid for a supply frequency lower than 150 Hz and a current lower than the critical current. For currents exceeding the material critical current, the impact of the resistive copper layers on the tape losses should be considered [22]. For frequencies higher than 150 Hz, magnetization losses in copper layers will no longer be negligible [23]. However, for the operative conditions considered in this study, the losses in the remaining conducting layers of the superconducting tape can be neglected.

The T-A formulation is applied in FEM by defining in the tape domain the potential vector **T** in (3).

$$\nabla \times \mathbf{T} = \mathbf{J} \quad (3)$$

In all other domains of the model, the magnetic vector potential **A** is defined as in (4).

$$\nabla \times \mathbf{A} = \mathbf{B} \quad (4)$$

These two equations can then be used to solve Faraday's law [24].

$$\nabla \times \mathbf{E} = -\frac{\partial \mathbf{B}}{\partial t} \quad (5)$$

To apply the current in the tape, Dirichlet boundary conditions are imposed at its edges. Since **T** can be obtained by integrating the current density **J** over the cross-section of the layer, then by Stokes theorem, the value for **T** at each edge of the tape T_1 and T_2 is obtained by (6) [25].

$$\iint_S \mathbf{J} \cdot \mathbf{n} dS = \iint_S (\nabla \times \mathbf{T}) \cdot \mathbf{n} dS = \oint_L \mathbf{T} dl = (T_1 - T_2)\delta \quad (6)$$

In (6), L denotes the path formed by the boundary edges of the conductor, and δ is the thickness of the superconductor.

IV. 2D Slot Model

The 2D slot model is based on the magnetic field information derived from a 3D FEM simulation of the complete electric machine. Considering the geometric symmetry of the machine, each slot will be subject to similar magnetic field evolution for a complete rotation of the rotor. Hence, for the analyses on the magnetic field surrounding the conductors, only a single slot has been analyzed, assuming similar conditions for all the others.

By means of preliminary 3D FEM simulations on the considered axial flux machine with copper conductors, it has been verified that the magnetic flux distribution into the slot is not significantly altered along the slot length in the machine radial coordinate, i.e., along the *z*-direction according to the reference frame reported in Fig. 4 and Fig. 6 [14]. This means that in the 3D FEM model, a single cut plane can be defined at the middle slot length to retrieve the information of the magnetic field acting on the slot edges. This information can then be applied to the cross-section model of the slot to perform straightforward analyses.

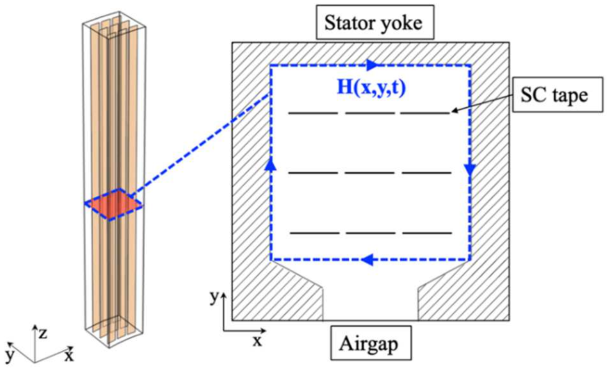

Fig. 6. Stator slot model in 3D (left) with highlighted in red the cut plane for defining the boundary conditions to be applied in the 2D slot model (right).

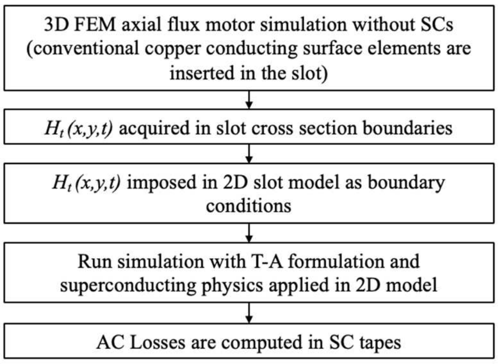

Fig. 7. Slot model methodology flow chart.

Therefore, the resulting SC losses obtained by the 2D single slot model can be extended to the whole machine, multiplying by the slot length and total number of stator slots.

Fig. 6 shows on its left side a 3D sketch of a stator slot with the 9 surface conducting elements, together with the cut plane for the slot cross-section definition (in red). For each mesh node lying on the boundaries of the slot cross-section (which is represented in the dashed blue line in Fig. 6), the tangential magnetic field $H_t(x,y)$ is obtained. Applying this procedure for each time step of a 3D transient FEM simulation, the time evolution of the magnetic field for each of the mesh nodes $H_t(x,y,t)$ is retrieved. Obviously, higher mesh densities and small time steps in the resolution of the 3D FEM model result in higher accuracy in the definition of the magnetic field on the slot edges. Despite the longer solving time for the initial 3D model, the enhanced accuracy in the magnetic field definition will reflect in more accurate analyses using the 2D single slot model.

In the 2D slot model, the acquired magnetic field is imposed as boundary condition for each mesh point on the slot edge. Since the mesh density that can be defined for 2D FEM models is usually thinner compared to those adopted in 3D models, and the time stepping shorter, the magnetic field information $H_t(x,y,t)$ obtained by the 3D analysis has to be interpolated for the remaining mesh nodes and time steps. At this point, since the magnetic field conditions have been defined, the conducting elements are modeled in the 2D slot model by applying the superconducting formulations reported in Section III.

It has to be noted that by defining the tangential component of the magnetic field along the slot borders, the total current inside the slot is also defined.

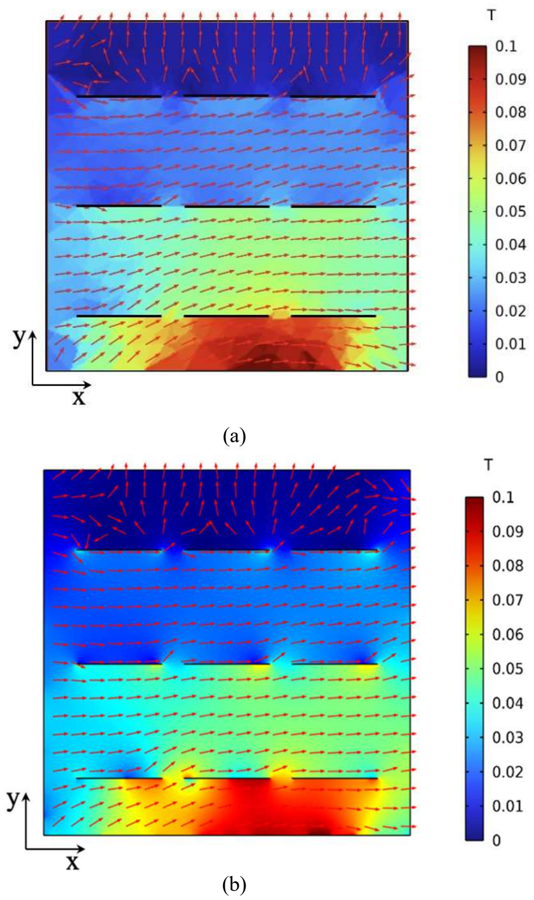

(a)

(b)

Fig. 8. Magnetic flux density color shade map and B_x, B_y surface plot arrows in the cut plane of the 3D machine slot (a), and in the 2D slot model (b).

The magnetic field on the full 3D machine and 2D slot model are the same, and by Ampère's law, the slot current is also the same. The full methodology for the superconductors AC loss estimation is summarized in the diagram in Fig. 7.

A. Numerical analyses

Figure 8 shows the color shade maps for the flux density norm |**B**| and the flux density arrow surface, B_x and B_y, in the analyzed stator slot. In detail, Fig. 8a shows the results on the slot cross-section defined by the cut plane in the 3D model of the complete machine with '*flat*' copper conductors. The simulation has been conducted considering both the rated current in the conductors and the permanent magnet magnetization. According to the procedure described the information on the magnetic field on the slot edges in the 3D model has then been imposed on the 2D slot model as boundary conditions, and the superconducting tapes were introduced. The results in terms of |**B**| color shade map and B_x and B_y arrows for the 2D single slot model with superconducting tapes are displayed in Fig. 8b.

By comparing the results in Fig. 8a and Fig. 8b, it is verified that the method used accurately describes the magnetic flux density in the 2D slot model, particularly in proximity to the conducting elements. The arrow plots in Fig. 8 also confirm that the magnetic leakage flux into the slot mainly flows straight through the slot width (x-direction according to the model reference system displayed in the figures), except for the top and bottom slot regions that are, respectively, affected by the presence of the slot opening and the stator yoke.

The results confirm the appropriateness of considering core-wound windings for realizing a superconducting axial flux machine. In fact, the tapes orientation into the stator slot that better matches the bending purposes around the stator core is shown in Fig. 1b and Fig. 4. This tape orientation also allows to maintain the magnetic flux density almost parallel to the tapes, significantly reducing the impact on the superconductor losses [26].

B. Losses estimation in SCs using the 2D single slot model and comparison with analytical methods

A superconductor carrying an AC current presents a non-negligible transport loss contribution (P_T). Similarly, when the superconductor is operated in the presence of an external magnetic field, it presents magnetization losses (P_M) [27]. The literature on superconductivity reports analytical formulations that are often used to estimate these loss components in SCs. In detail, the Norris equation is used for the transport losses, while the Brandt formulation is applied for magnetization losses [28], [29]. Therefore, these analytical formulations are here considered for assessing the accuracy of the proposed 2D single slot model in estimating the losses in superconducting tapes when used for AC windings of electrical machines.

However, it has to be considered that Norris's formulation is valid only for SCs with AC transport currents and in self-field conditions, while Brandt's formulation is valid for SCs immersed in a time-varying magnetic field but without transport current into the conductor. For this purpose, two analyses were done using the developed FEM models. The first one aims at determining only the magnetization loss component that originates from the magnetic flux produced by the permanent magnets on the machine and that invests the superconducting tapes positioned into the stator slot. In this case, the magnetic field is determined from the 3D AFPM model when the machine slot current is set to zero, and the permanent magnets have a remanent flux density B_r = 1.1 T. The second case analyzed aims to determine the transport loss component. In this case, the FEM model is simulated by applying the rated current to the superconductors and no magnetic field from the permanent magnets. This is done by setting the magnet remanence B_r to zero and imposing a rated slot current of 910 A in all slots.

The magnetic field amplitude perpendicular to each tape surface (y direction in Fig. 8) is evaluated to compute the analytical losses P_M (W/m) given by Brandt's equation for magnetization losses [29]. This solution, for a superconducting strip subject to an alternate external magnetic field applied perpendicular to the tape, is stated in (7).

$$P_M = \mu_0 w^2 f J_c \delta H_0 g\left(\frac{H_0}{H_c}\right) \quad (7)$$

In (7), w is the superconductor width, f is the frequency of the applied magnetic field and H_0 is its amplitude, H_c is the characteristic field, $I_{c0}/w\pi$, and $g(x)$ is given by (8).

$$g(x) = (2/x)\ln\cosh(x) - \tanh(x) \quad (8)$$

For the simulation where only applied current is considered, the transport loss analytical solution P_T (W/m) is given by Norris' equation for a tape carrying an AC current in its hysteretic stage [28]. The solution is stated in (9).

$$P_T = \frac{\mu_0 f I_{c0}^2}{\pi}\left[(1-i)\ln(1-i) + (1+i)\ln(1+i) - i^2\right] \quad (9)$$

TABLE III. FEM AND ANALYTICAL AC LOSSES

Model	FEM	Analytical	
	2D Slot model (W/m)	P_T (W/m)	P_M (W/m)
Applied current	0.273	0.234	-
Applied field	0.134	-	0.118

TABLE IV. 2D VS. 3D LOSSES AND SIMULATION TIME

Slot model	P (W/m)	Simulation time
2D [14]	2.09	3m 50s
2D	1.24	20m 40s
3D	1.52	14h 28m 51s

In (9), i is the ratio between the transport current and the critical current at self-field, I_t/I_{c0} and f is the frequency of the supply current. In the FEM model, the tape losses per unit length P (W/m) are determined by the time integration of the instantaneous AC loss over one cycle (10).

$$p(t) = \int_w E \cdot (J\delta) dw$$
$$P = \frac{1}{T}\int_0^T p(t)dt \quad (10)$$

Table III reports the analytical solutions with the slot model results, showing coherent values and validating the 2D model.

V. 3D SINGLE SLOT MODEL

To further verify the accuracy of the 2D slot model approach in evaluating the SC losses, the methodology has also been extended to a 3D single-slot model. In detail, from the 3D FEM model of the complete AFPM machine initially solved with copper conductors, the magnetic field distribution is derived, in each mesh point in the x, y, z coordinates of the analyzed armature slot, and for all the simulation time instants. The resulting matrix $H_t(x,y,z,t)$ is applied to the 3D single slot model through magnetic field boundary conditions, and the T-A formulation is used for modeling the superconducting tapes.

The AC losses evaluated for the nine SC tapes using the 2D and the 3D single slot models are listed in Table IV. The computing time for the expanded 2D model proposed in this paper is higher due to its detailed magnetic field representation compared to the model in [14]. However, applying the expanded 2D model reduces the relative error to the 3D model from 38% in [14] to 18%. The losses estimated by the expanded 2D model are lower than those from the 3D simulation and the method in [14]. Nonetheless, the expanded model shows consistency in the magnetic field representation with the result obtained in the 3D model, which is essential for evaluating superconducting tape performance.

The 2D model provides the advantage of lower computation time, while the 3D model presents a more rigorous magnetic field representation. The difference between the 2D and the 3D models can be attributed to using different meshes and the time stepping in each model. Note that the end-windings are not included since this model is only used to evaluate the losses inside the slot region. When the end-windings are included in the 3D model, the magnetic field surrounding the tapes outside the slot region will no longer be parallel to the conductor surfaces, and most likely, this will cause an increase in losses in the superconductors.

VI. CONCLUSION

This paper presents a method for expediting loss computation considering superconducting AC windings in electrical machines that, for their geometrical nature, require 3D simulation models. Specifically, the 2D slot model previously developed in [14] is expanded to provide a more accurate description of the magnetic field time- and spatial harmonics in the stator slot of AC electrical machines. The proposed 2D modeling approach allows to restrict the FEM simulation only to the slot and the SC elements, avoiding dealing with moving mesh for the rotor and other non-linear materials such as the laminated iron core.

The full machine is first simulated in 3D using applied currents on surface copper conducting elements. The information about the tangential magnetic field along the slot edges and its time variation is derived and applied to the 2D single slot model, where SCs are modeled using the *T-A* formulation. As case study, this research uses a preliminary-sized axial flux permanent magnet motor with superconducting stator winding. The proposed method is validated by comparing the estimated transport and magnetization losses in the superconducting tapes with those computed by analytical formulations reported in the literature. This methodology provides an efficient procedure for loss estimation in the design of superconducting AC electrical machines, and it can be used to estimate the cooling power required for superconducting AC windings. Furthermore, the 2D single slot model can also be exploited to investigate practical methods to mitigate the effects of the applied magnetic field on the SC tapes, such as shields, flux diverters, and different tapes positioning inside the armature slot.

REFERENCES

[1] G. Sarmiento, S. Sanz, A. Pujana et al., “Design and Testing of Real-Scale MgB2 Coils for SUPRAPOWER 10-MW Wind Generators,” in *IEEE Trans. Appl. Supercond.*, vol. 26, no. 3, pp. 1-6, April 2016.

[2] H. Kyling, N. Eich and P. Feja, “Measuring MNm torques as part of a prototype testing campaign of a high-temperature superconducting generator for wind turbine application in the scope of the Ecoswing project,” J. Phys.: Conf. Ser., vol. 1222, pp. 012018, April 2019.

[3] “SEA-TITAN Surging Energy Absorption Through Increasing Thrust And efficieNcy European Commission.” [Online]. Available https://cordis.europa.eu/project/id/764014. Accessed on: March 5, 2024.

[4] Y. Wang, F.Weng, J. Li et al., "No-Insulation High-Temperature Superconductor Winding Technique for Electrical Aircraft Propulsion," in *IEEE Trans. Transp. Electrif.*, vol. 6, no. 4, pp. 1613-1624, Dec. 2020.

[5] “ASuMED: Advanced Superconducting Motor Experimental Demonstrator European Commission.” [Online]. Available https://cordis.europa.eu/project/id/723119/. Accessed on: Mar. 5, 2024.

[6] W. Stautner, P. J. Ansell and K. S. Haran, "CHEETA: An All-Electric Aircraft Takes Cryogenics and Superconductivity on Board: Combatting climate change," *IEEE Electrif. Mag.*, vol. 10, no. 2, pp. 34-42, June 2022.

[7] M. Biasion, J. F. P. Fernandes, S. Vaschetto, A. Cavagnino and A. Tenconi, “Superconductivity and its Application in the Field of Electrical Machines,” 2021 IEEE International Electric Machines & Drives Conference (IEMDC), Hartford, CT, USA, 2021, pp. 1-7.

[8] C. C. T. Chow, M. D. Ainslie, K. T. Chau, “High temperature superconducting rotating electrical machines: An overview,” Energy Reports, vol. 9, pp. 1124-1156, 2023.

[9] B. M. O. Santos, F. J. M. Dias, G. G. Sotelo and R. de Andrade Junior “A Review of Technology Readiness Levels for Superconducting Electric Machinery,” *Energies*, vol. 16, pp. 5955, 2023.

[10] H. Zhang, Z. Wen, F. Grilli, K. Gyftakis and M. Mueller, “Alternating Current Loss of Superconductors Applied to Superconducting Electrical Machines,” *Energies*, vol. 14, pp. 2234, 2021.

[11] D. J. Gameiro Carvalho, F. Ferreira da Silva, J. F. P. Fernandes and P. J. da Costa Branco, “Finite-element recipes for HTS-coated conductors and HTS tape topologies,” *Supercond. Sci. Technol.*, vol. 36, no. 10, 2023.

[12] I. S. P. Peixoto, F. F. da Silva, J. F. P. Fernandes, S. Vaschetto and P. J. C. Branco, "A Distributed Equivalent-Permeability Model for the 3-D Design Optimization of Bulk Superconducting Electromechanical Systems," in *IEEE Trans. Appl. Supercond.*, vol. 33, no. 6, pp. 1-10, Sept. 2023, Art no. 3601610.
[13] L. Hao, F. Dong, J. Hu et al. "3D Electromagnetic Modelling for High-temperature Superconducting Dynamo Flux Pumps Using T-A Formulation," High voltage, 1–13, 2024.
[14] I. S. P. Peixoto, S. Vaschetto, J. F. P. Fernandes, P. J. Da Costa Branco, A. Tenconi and A. Cavagnino," Modeling Approach for Superconducting AC Windings: Case Study on Axial Flux PM Machines," 2023 IEEE Energy Conversion Congress and Exposition (ECCE), Nashville, TN, USA, 2023, pp. 3790-3795.
[15] S. Vaschetto, A. Tenconi and G. Bramerdorfer, "Sizing procedure of surface mounted PM machines for fast analytical evaluations," 2017 IEEE International Electric Machines and Drives Conference (IEMDC), Miami, FL, USA, 2017, pp. 1-8.
[16] SuperPower Inc., [Online]. Available: http://www.superpower-inc.com
[17] D. X. Chen; R. B. Goldfarb, "Kim model for magnetization of type-II superconductors," *J. Appl. Phys.*, vol. 66, pp. 2489–2500, 1989.
[18] D. A. Cardwell, D. C. Larbalestier, A. Braginski, Handbook of Superconductivity: Characterization and Applications, 2nd ed., vol.3 CRC Press, 2022.
[19] D. W. Hazelton and V. Selvamanickam, "SuperPower's YBCO Coated High-Temperature Superconducting (HTS) Wire and Magnet Applications," in Proc. IEEE, vol. 97, no. 11, pp. 1831-1836, Nov. 2009.
[20] H. Tsuboi, and K. Kunisue, "Eddy Current Analysis of Thin Plates Taking Account of the Source Current Distributions and Its Experimental Verifications," in *IEEE Trans. Magn.*, vol.27 pp. 4020–4023, 1991.
[21] M. Nii, N. Amemiya, and T. Nakamura, "Three-Dimensional Model for Numerical Electromagnetic Field Analyses of Coated Superconductors and Its Application to Roebel Cables," *Supercond. Sci. Technol.* vol.25 pp. 95011, 2012.
[22] J. F. P. Fernandes, L. F. D. Bucho, F Ferreira da Silva1, I. S P Peixoto, S. Vaschetto and P J Costa Branco, "Alternative analytical models for HTS tapes considering their AC hysteretic and resistive losses," *Supercond. Sci. Technol.* vol. 37 pp. 035004.
[23] H. Zhang, M. Yao, K. Kails et al., "Modelling of electromagnetic loss in HTS coated conductors over a wide frequency band," *Supercond. Sci. Technol.*, vol. 33, pp. 025004, 2020.
[24] F. Huber, W. Song, M. Zhang, and F. Grilli, "The T-A formulation: an efficient approach to model the macroscopic electromagnetic behaviour of HTS coated conductor applications," *Supercond. Sci. Technol.*, vol. 35, pp. 043003, 2022.
[25] E. Berrospe-Juarez, V. M. R. Zermeño, F. Trillaud and F. Grilli, "Real-Time Simulation of Large-Scale HTS Systems: Multi-Scale and Homogeneous Models Using the T-A Formulation." *Supercond. Sci. Technol.*, vol.32 pp. 65003, 2019.
[26] N. Amemiya, Z. Jiang, Y. Iijima, K. Kakimoto and T. Saitoh, "Total AC loss of YBCO coated conductor carrying AC transport current in AC transverse magnetic field with various orientations," *Supercond. Sci. Technol.,* vol. 17, pp. 983, Jun. 2004.
[27] J. J. Rabbers, D. C. van der Laan, B. ten Haken and H. H. J. ten Kate, "Magnetisation and transport current loss of a BSCCO/Ag tape in an external AC magnetic field carrying an AC transport current," in *IEEE Trans. Appl. Supercond.*, vol. 9, no. 2, pp. 1185-1188, June 1999.
[28] W. T. Norris, "Calculation of hysteresis losses in hard superconductors carrying ac: isolated conductors and edges of thin sheets," *J. Phys. D: Appl. Phys.*, vol.3, pp. 489, April 1970.
[29] E. H. Brandt, and M. Indenbom, "Type-II-superconductor strip with current in a perpendicular magnetic field," *Phys. Rev. B*, vol. 48, pp. 12893–12906, Nov. 1993.

Inês Peixoto (S'21) received the M.Sc. degree in electrical and computers engineering from Instituto Superior Técnico (IST), Portugal, in 2020. She joined Politecnico di Torino as a PhD student in 2021, starting her research activity on the application of superconductors in new designs of electric machines for the electric energy conversion at very high efficiency and specific power. Her work is focused in using experimental characterization of ferromagetic and superconducting materials at cryogenic conditions to develop multiphysics models for estimation of superconductors performance in electrical machines' armature windings.

Lorenzo Perilli (S'24) received the B.Sc. degree in Industrial Engineering from Università degli Studi dell'Aquila, Italy, and the M.Sc. degree in Electrical Engineering from Politecnico di Torino, Italy, in 2020 and 2023, respectively. He is currently working toward the Ph.D. degree in Electrical Engineering with the Department of Energy "G. Ferraris," at Politecnico di Torino. His research activity focuses on electric machines design and modeling for the aircraft electrification.

Federica Graffeo (S'20-M'24) received the B.Sc. degree in Energy Engineering from Università degli Studi di Palermo (Italy) in 2017, the M.Sc. and Ph.D. degree in Electrical Engineering from Politecnico di Torino (Italy) in 2020, and 2023, respectively. She is currently Assistant Professor with Dipartimento Energia "G. Ferraris," Politecnico di Torino. She serves as a reviewer for some IEEE Transactions and international conferences. Her main research interests include electromagnetic and thermal design of synchronous electrical machines for transportation applications, with a particular focus on wound field synchronous motors.

João Fernandes (M'20) received the M.Sc. and Ph.D. degrees in electrical and computers engineering from the Instituto Superior Técnico, Portugal, in 2011 and 2017, respectively. He was a partner of start-up Emove, Innovative Technologies, Lda from 2008 to 2014 and was an electrical engineer at Efacec Engenharia from 2011 to 2013. He is currently an Assistant Professor of Electrical and Computers Engineering at Instituto Superior Técnico and an integrated member of IDMEC/LAETA. His research focuses on expanding the current limits of electrical machines, using emerging advanced electromagnetic materials, such as superconductors, and design methodologies. He is an Associate Editor for IEEE TRANSACTIONS ON ENERGY CONVERSION, serves as guest editor in two Special Issues, and he is the current secretary of the Portuguese section of IEEE Power & Energy Society (PES).

Paulo Branco (M'92) received the M.Sc., Ph.D. dnd Habilitation in electrical engineering from Instituto Superior Técnico (IST), Portugal, in 1992, 1998, and 2013, respectively. In 1992, he joined ST as a Trainee Assistant for the Electrical Machines and Power Electronics (SMEEP) Section of the Department of Electrical and Computer Engineering (DEEC). In 1993, became Assistant Professor, and in 2005 became an Associate Professor in the same place. Currently, he is a Full Professor (IST, 2023) at DEEC. His research interests are using superconducting materials in electrical machines, operating induction generators when isolated from the power grid and at a variable speed in the pump as working turbines (PATs), and criticality in the smart grid operation environment. He is Chair of the IEEE Portugal Power and Energy Society (PES) Section, 2024/25; Vice-Coordinator of the Center for Intelligent Systems, IDMEC, LAETA (Lab. Ass. in Energy, Transport and Aeronautics); 3), and member of the IEEE Council on Superconductivity as representative of IEEE POWER & ENERGY SOCIETY (IEEE PES).

Silvio Vaschetto (S'10–M'13–SM'19) received the M.Sc. and Ph.D. degrees in electrical engineering from the Politecnico di Torino, Italy, in 2007 and 2011, respectively. He then joined ABB IEC LV Motors Technology Center, Vittuone, Italy as R&D engineer. From 2012 to 2014 he was with Magna Electronics Italy, as Electromagnetic Simulation and Motor Design Engineer. He is currently an Associate Professor at the Energy Department "G. Ferraris", Politecnico di Torino. His research interests include electromagnetic design, thermal design, and energetic behavior of electrical machines for transportations and high-performance applications. He is an Associate Editor for IEEE TRANSACTIONS ON INDUSTRY APPLICATIONS, IEEE TRANSACTIONS ON ENERGY CONVERSION and Special Issues Editor for IET *Electric Power Applications Journal.*